

# Optimal Radio Window for the Detection of Ultra-High-Energy Cosmic Rays and Neutrinos off the Moon.

O. Scholten,<sup>1,\*</sup> J. Bacelar,<sup>1</sup> R. Braun,<sup>2</sup> A.G. de Bruyn,<sup>2,3</sup> H. Falcke,<sup>2,4</sup> B. Stappers,<sup>2,5</sup> and R.G. Strom<sup>2,5</sup>

<sup>1</sup>*Kernfysisch Versneller Instituut, University of Groningen, 9747 AA, Groningen, The Netherlands*

<sup>2</sup>*ASTRON, 7990 AA Dwingeloo, The Netherlands*

<sup>3</sup>*Kapteyn Institute, University of Groningen, 9747 AA, Groningen, The Netherlands*

<sup>4</sup>*Department of Astrophysics, IMAPP, Radboud University, 6500 GL Nijmegen, The Netherlands*

<sup>5</sup>*Astronomical Institute 'A. Pannekoek', University of Amsterdam, 1098 SJ, The Netherlands*

When high-energy cosmic rays impinge on a dense dielectric medium, radio waves are produced through the Askaryan effect. We show that at wavelengths comparable to the length of the shower produced by an Ultra-High Energy cosmic ray or neutrino, radio signals are an extremely efficient way to detect these particles. Through an example it is shown that this new approach offers, for the first time, the realistic possibility of measuring UHE neutrino fluxes below the Waxman-Bahcall limit. It is shown that in only one month of observing with the upcoming LOFAR radio telescope, cosmic-ray events can be measured beyond the GZK-limit, at a sensitivity level of two orders of magnitude below the extrapolated values.

## I. INTRODUCTION

The interest in determining the flux of Ultra-High Energy (UHE) cosmic rays and neutrinos is manifold. The origin of the highest energy cosmic rays is a major research topic as the existence of these particles requires very spectacular events on a cosmic scale. At energies beyond the so-called Greisen-Zatsepin-Kuzmin (GZK)-limit [1, 2] (at an energy of about  $6 \cdot 10^{19}$  eV) the spectrum of cosmic rays is expected to drop rather drastically. The mechanism for this is that at these energies the cosmic rays produce pions when scattering off the microwave background while traversing distances of the order of 10 Mpc. The existence of this cutoff in the spectrum has not been verified unambiguously up to now. The flux of cosmic rays beyond the GZK cutoff determines the sources for UHE cosmic rays within a range of about 10 Mpc [3, 4] i.e. close on astronomical scales. This is a very exciting prospect as presently there are no known sources at this proximity. The presently proposed method is very efficient for determining this flux.

Another point of interest lies in the detection of UHE neutrinos. These could be created by UHE protons producing  $\pi^+$  mesons when scattering off the microwave background (the GZK mechanism as mentioned above) which, through weak decay, produce neutrinos. These GZK neutrinos have thus far never been observed.

There are also other, more speculative, models predicting UHE neutrinos. These models belong to a generic class known as top-down (TD) models, where UHE particles owe their origin to the decay of some supermassive X-particle of mass  $m_X$ . Their decay products, the UHE-cosmic rays, can have energies up to  $m_X$ . These massive X particles could be topological defects or magnetic monopoles that could be produced in the early Universe

during symmetry-breaking phase transitions envisaged in grand unified theories (GUTs); see [5, 6, 7, 8] for reviews.

As an efficient method to determine the fluxes of UHE particles we are investigating the production of radio waves in a particular frequency window when a UHE particle hits the moon. Askaryan predicted as early as 1962 [9] that particle showers in dense media produce coherent pulses of microwave Čerenkov radiation. Recently this prediction was confirmed in experiments at accelerators [10] and extensive calculations have been performed on the development of showers in dense media to yield quantitative predictions for this effect [11]. The Askaryan mechanism lies at the basis of several experiments to detect (UHE) neutrinos using the Čerenkov radiation emitted in ice caps [12, 13], salt layers [14], and the lunar regolith. The pulses from the latter process are detectable at Earth with radio telescopes, an idea first proposed by Dagkesamanskii and Zheleznyk [15] and later by others [16]. Several experiments have since been performed [17, 18] to find evidence for UHE neutrinos. All of these experiments have looked for this coherent radiation near the frequency where the intensity of the emitted radio waves is expected to reach its maximum. Since the typical lateral size of a shower is of the order of 10 cm the peak frequency is of the order of 3 GHz.

Here we propose a different strategy to look for the radio waves at considerably lower frequencies where the wavelength of the radiation is comparable in magnitude to typical longitudinal size of showers. It has been noted before [18] that a new generation of low-frequency digital radio telescopes will provide excellent detection capabilities for high-energy particles, thus making our consideration here very timely. We show that the lower intensity of the emitted radiation, which implies a loss in detection efficiency, is compensated by the increase in detection efficiency due to the near isotropic emission of coherent radiation. The net effect is an increased sensitivity by several orders of magnitude, for the detection of UHE cosmic rays and neutrinos at frequencies which are one

---

\*Electronic address: scholten@kvi.nl

or two orders of magnitude below that where the intensity reaches its maximum. At lower frequencies the lunar regolith becomes increasingly transparent for radio waves. This implies for the detection of UHE neutrinos that there are two gain factors when going to lower energies; i) Increased transparency of the lunar regolith already stressed in Ref. [19], and ii) Increased angular acceptance, stressed in this work, which gives much larger count rates.

In the following two sections we explain quantitatively the idea of an optimum frequency by taking cosmic-ray and neutrino-induced radio-emission from the Moon as a specific example. The advantage of going to lower frequencies also applies to other experiments where the radiation crosses a boundary between a dense medium to one with a considerably lower index of refraction. In Section IV we propose two specific observations, one for an existing facility, the Westerbork Synthesis Radio-Telescope array (WSRT), and one for a facility which will be available in the near future, the Low-Frequency Array (LOFAR).

## II. MODEL FOR RADIO EMISSION

There exist two rather different mechanisms for radio emission from showers triggered by UHE cosmic rays or neutrinos, where each has received considerable attention recently. One is the emission of radio waves from a shower in the terrestrial atmosphere. Here the primary mechanism is the synchrotron acceleration of the electrons and positrons in the shower due to the geomagnetic field, called geosynchrotron radiation, which has recently been confirmed with new digital radio techniques [19, 20, 21, 22, 23]. The second mechanism applies to showers in dense media, such as ice, salt, and lunar regolith, where the front end of the shower has a surplus of electrons. Since this cloud of negative charge is moving with a velocity which exceeds the velocity of light in the medium, Čerenkov radiation is emitted. For a wavelength of the same order of magnitude as the typical size of this cloud, which is in the radio-frequency range, coherence builds up and the intensity of the emitted radiation reaches a maximum. This process, known as the Askaryan effect [9] is the subject of this paper.

The intensity of radio emission (expressed in units of Jansky's where  $1 \text{ Jy} = 10^{-26} \text{ W m}^{-2}\text{Hz}^{-1}$ ) from a hadronic shower, with energy  $E_s$ , in the lunar regolith, in a bandwidth  $\Delta\nu$  at a frequency  $\nu$  and an angle  $\theta$ , can be parameterized as (see Appendix A)

$$F(\theta, \nu, E_s) = 3.86 \times 10^4 e^{-Z^2} \left( \frac{\sin \theta}{\sin \theta_c} \right)^2 \left( \frac{E_s}{10^{20} \text{ eV}} \right)^2 \times \left( \frac{d_{\text{moon}}}{d} \right)^2 \left( \frac{\nu}{\nu_0(1 + (\nu/\nu_0)^{1.44})} \right)^2 \left( \frac{\Delta\nu}{100 \text{ MHz}} \right) \text{ Jy}, \quad (1)$$

with

$$Z = (\cos \theta - 1/n) \left( \frac{n}{\sqrt{n^2 - 1}} \right) \left( \frac{180}{\pi \Delta_c} \right), \quad (2)$$

where  $\nu_0 = 2.5 \text{ GHz}$  [18],  $d$  is the distance to the observer, and  $d_{\text{moon}} = 3.844 \times 10^8 \text{ m}$  is the average Earth-Moon distance. The angle at which the intensity of the radiation reaches a maximum, the Čerenkov angle, is related to the index of refraction ( $n$ ) of the medium,  $\cos \theta_c = 1/n$ . Crucial for our present discussion is the spreading of the radiated intensity around the Čerenkov angle, given by  $\Delta_c$  (in degrees). The  $\sin \theta$  factor in Eq. (1) reflects the projection of the velocity of the charges in the shower on the polarization direction of the emitted Čerenkov radiation. The dependence of  $Z$  as defined in Eq. (2) is suggested by working out some specific cases [12], see Appendix A. For small values of  $\Delta_c$  it coincides with the formula Eq. (A1) found in much of the literature [11, 16, 18] however, Eq. (1) is more accurate for large spreading angles.

The spreading of the radiated intensity around the Čerenkov angle,  $\Delta_c$ , is, on the basis of general physical arguments, inversely proportional to the shower length and the frequency of the emitted radiation. Based on the results given in Ref. [16] it can be parameterized as

$$\Delta_c = 4.32^\circ \left( \frac{1}{\nu [\text{GHz}]} \right) \left( \frac{L(10^{20} \text{ eV})}{L(E_s)} \right), \quad (3)$$

where  $L(E_s)$  is the shower length which depends on the energy. In Ref. [27], calculated results are given for the shower length (in units of radiation lengths, equal to  $22.1 \text{ g/cm}^2$  [43] for lunar regolith) which at the highest energies can be parameterized as

$$L(x) = 12.7 + \frac{2}{3}x, \quad (4)$$

where  $x = \log_{10}(E/10^{20} \text{ eV})$ . At an energy of  $10^{20} \text{ eV}$  this corresponds to a shower length of approximately 1.7 m, where we take the density of the regolith to be approximately  $1.7 \text{ g/cm}^3$ . For a frequency  $\nu = 200 \text{ MHz}$ , where the wavelength is of the same order as the shower length, we should expect on general arguments that the radiation spreads over an angular range ( $2\Delta_c$ ) that is comparable to the Čerenkov angle,  $\theta_c = 56^\circ$ . This indeed corresponds to the value  $\Delta_c = 21.52^\circ$ , obtained from Eq. (3). In Appendix A the predictions for the angular spread based on the parametrization Eq. (1) using Eq. (3) is compared with analytical calculations for some (simplified) shower profiles showing excellent consistency with the calculated shower length.

In our simulations we have taken into account the attenuation of radio waves in the regolith. As a mean value for the attenuation length for the radiated power we have taken  $\lambda_r = (9/\nu[\text{GHz}]) \text{ m}$  [24], which is the same value as used in the analysis of the GLUE experiment [18]. This value is obtained from loss-tangent measurements performed on samples of lunar basalt brought back from the Moon [24]. The measured values show a rather large variation, the effects of which are investigated in Section V. In principle the layer of regolith is only 10-20 m thick under which there a thick layer of fractured rock

going over into solid bedrock. As shown in Appendix C the bedrock is as efficient in emitting radio waves at the lower frequencies as the regolith. At higher frequencies, due to the larger attenuation length, only the relatively thin upper layer contributes to radio emission. All in all this implies that for the calculation of the acceptance the structure of the deeper layers (rock v.s. regolith) is not important. In the calculations we have therefore included radiation coming from a depth of at most 500 m treating for simplicity, and without loss of accuracy, the whole layer as behaving like regolith. It is argued in Appendix C that this indeed gives a realistic estimate for the acceptance calculations.

In the calculations for cosmic-ray-induced showers we assumed that the shower occurs effectively at the lunar surface. As argued in Appendix B only a very small depth is necessary for Čerenkov radiation to be emitted. For neutrino-induced showers an energy-dependent mean free path [25] has been used,  $\lambda_\nu = 130 \left( \frac{10^{20} \text{ eV}}{E_\nu} \right)^{1/3}$  km which is appropriate for regolith.

A crucial point in the simulation is the refraction of radio waves at the lunar surface as was already stressed in Ref. [11]. Since the index of refraction of the lunar regolith is relatively large,  $n = 1.8$  corresponding to a Čerenkov angle of  $\theta_c = 56^\circ$ , much of the radio wave which is emitted by the shower suffers internal reflection at the surface. Only radiation with an angle of  $90^\circ - \theta_c$  or less with respect to the normal to the surface will be emitted from the Moon. Since most showers, being cosmic ray or neutrino induced, are directed towards the center of the Moon, internal reflection will severely diminish the emitted radiation at high frequencies where the Čerenkov cone is rather narrow. The major advantage of going to lower frequencies is that the spreading  $\Delta_c$  around  $\theta_c$  increases, allowing for the radiation to escape from the lunar surface. With decreasing frequency the peak intensity of the emitted radiation decreases (see Eq. (A1)), however the peak intensity increases with increased particle energy. The net effect is that at sufficiently high shower energies the aforementioned effect of increased spreading is far more important, resulting in a strong increase in the detection probability.

To be able to address these issues quantitatively we introduce the detection efficiency  $\mathcal{D}(E, \nu)$ . It is defined as the probability that a cosmic ray (or neutrino) hitting the Moon (at an arbitrary angle and position) with energy  $E$  would produce radio waves at frequency  $\nu$  which is detectable at Earth. We regard an event to be detectable when the power of the signal is 25 times larger than the “noise level” which we take equal to  $F_{noise} = 20$  Jy [26], i.e. a minimal detection level of 500 Jy is taken using a bandwidth of  $\Delta\nu = 20$  MHz in Eq. (1). These values can be considered typical for LOFAR, see Section IV. It is illustrative to plot the differential detection probability,  $d\mathcal{D}/d\Omega$ , for a particular area  $dA = R^2 d\Omega$  on the Moon where  $R$  is the lunar radius. In Fig. 1,  $d\mathcal{D}/d\Omega$  is plotted for cosmic rays at an energy of  $4 \times 10^{21}$  eV for

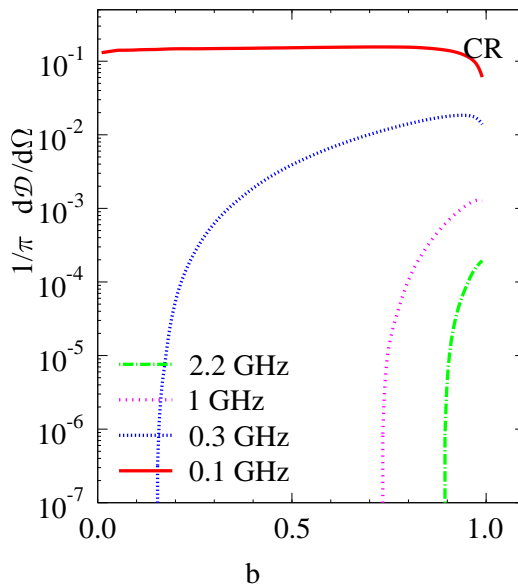


FIG. 1: Differential detection probability,  $d\mathcal{D}/d\Omega$ , for a cosmic ray of energy  $4 \times 10^{21}$  eV hitting the Moon as function of apparent distance from the center of the Moon,  $b$ , for different detection frequencies.

TABLE I: Calculated detection probabilities for cosmic-ray induced showers at  $E_{cr} = 4 \times 10^{21}$  eV, labelled as  $\mathcal{D}_{cr}(40)$ , and for neutrino-induced showers at  $E_\nu = 2 \times 10^{22}$  eV, labelled as  $\mathcal{D}_\nu(200)$ , for different frequencies  $\nu$  (in units of GHz).

$\nu$	$\mathcal{D}_{cr}(40)$	$\mathcal{D}_\nu(200)$
2.2	$1.92 \times 10^{-5}$	$3.03 \times 10^{-7}$
1.0	$2.65 \times 10^{-4}$	$4.85 \times 10^{-6}$
0.3	$9.84 \times 10^{-3}$	$1.97 \times 10^{-4}$
0.1	$1.44 \times 10^{-1}$	$2.92 \times 10^{-3}$

different frequencies as a function of the relative distance from the center of the face of the Moon,  $b$ , where  $b = 1$  corresponds to the rim of the Moon. At lower frequencies the length of the shower becomes comparable to the wavelength of the radiation. Coherent emission of radio waves thus happens over a large angular range instead of only within a narrow cone at the Čerenkov angle. The effect of this is that even cosmic rays hitting the center of the face of the Moon (as seen by us) at very oblique angles are detectable. If the radiation were emitted in a very narrow cone around the Čerenkov angle, much of the radiation, even if the cone is directed towards the Earth, would be internally reflected off the lunar surface. All this implies that at high frequencies only the rim of the Moon contributes to  $d\mathcal{D}/d\Omega$  and that this contribution is not really large since only very inclined cosmic rays may produce detectable emission. At lower frequencies the whole surface of the Moon contributes with a relatively large probability since a large range of angles contribute. This trend is clearly discernable in Fig. 1.

In Table I the detection probabilities,  $\mathcal{D}$  ( $d\mathcal{D}/d\Omega$  integrated over the lunar surface), are given as a func-

tion of frequency. This shows a strong increase of  $\mathcal{D}$  with decreasing frequency. For a given shower the radiation that is transmitted through the surface (which is not internally reflected) is proportional to  $\Delta_c^2$ , where the quadratic dependence is due to the fact that the phase space is in both the polar and in the azimuthal angle. An additional factor of  $\Delta_c$  comes from the fact that also for showers making an angle of up to  $\Delta_c$  with respect to the tangent to the surface, radio waves may be transmitted through the surface. In total one expects thus  $\mathcal{D} \propto \Delta_c^3 \propto \nu^{-3}$  which agrees rather well with the numbers given in Table I.

For neutrino-induced showers only 20% of the initial energy is converted to a hadronic shower, while the remaining 80% is carried off by the lepton. This energetic lepton will not induce a detectable radio shower. For a muon, the density of charged particles will be too small, while the shower of a UHE electron will be extremely elongated due to the Landau-Pomeranchuk-Migdal effect [27]. The width of the Čerenkov cone will thus be very small which makes the shower practically undetectable. For the present calculations we therefore have limited ourselves to the hadronic part of the shower which carries 20% of the energy of the original neutrino. To be able to compare the results for cosmic-ray and neutrino-induced showers in Table I the latter have been calculated for a 5-times higher energy of the incoming particle.

While the showers for hadronic cosmic rays develop very close to the lunar surface, those of UHE neutrinos are distributed over a rather large range of depths from the surface. As a result of the long attenuation length for neutrinos in matter (tens of km at our energies), a large fraction of the neutrinos create showers too deep inside the Moon so that the radio waves are attenuated to below the detectable threshold at Earth. Roughly, one thus expects that the  $\mathcal{D}$  for neutrino-induced showers will be a factor  $\lambda_r/\lambda_\nu$  smaller than  $\mathcal{D}$  for cosmic-ray-induced showers at the same shower energy. This factor explains much of the difference between  $\mathcal{D}_{cr}$  and  $\mathcal{D}_\nu$  given in Table I.

A deviation from the simple  $\lambda_r/\lambda_\nu$  scaling occurs since, due to the relatively long neutrino mean free path, the hadronic part of the neutrino-induced shower has a certain probability of being directed towards the surface (in contrast to showers induced by hadronic cosmic rays which are always directed into the Moon). This increases the probability that part of the radio signal is emitted from the Moon. The latter can be seen from Fig. 2 where at 2.2 GHz the acceptance ring is broader than in Fig. 1.

An additional advantage of using lower frequencies is that the sensitivity of the model simulations to large- or small-scale surface roughness is diminished. Since at lower frequencies already a sizable fraction of the radiation penetrates the surface, its roughness will not make a major difference. This is in contrast to high frequencies where most of the radiation is internally reflected when surface roughness is ignored.

The increased spreading of the radiation around the

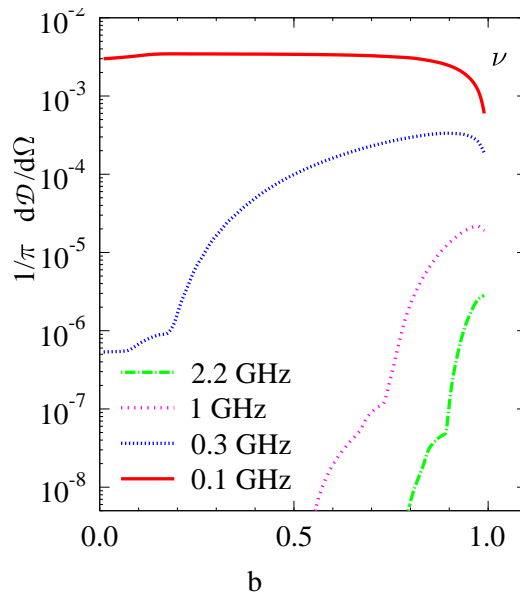


FIG. 2: Same as Fig. 1 but for showers induced by a neutrino of energy  $2 \times 10^{22}$  eV. It is assumed that 20% of the neutrino energy is deposited in a hadronic shower, the shower induced by the high-energy lepton is ignored in the present calculation since its Čerenkov cone is very sharp and thus a negligible fraction of its energy will penetrate through the lunar surface.

Čerenkov cone at lower frequencies strongly increases the detection efficiency but at the same time decreases the sensitivity to the direction of the original cosmic ray or neutrino. Part of this can be recovered by measuring the polarization direction of the radio waves. The electric field is 100% polarized in the direction of the shower, which has been confirmed in laboratory experiments [10].

### III. DETECTION LIMITS

In Fig. 3 the detection limits for UHE cosmic rays for different radio-frequency ranges are compared with data from the AGASA [28] (points) and a linear extrapolation based on the data from the HiRes experiment [29] (grey bar). The model-independent limit is defined as  $dN/dE_{lim} = Q/(\mathcal{D} \times h)$  where  $h$  equals the observation time in hours and  $Q = 1.16 \times 10^{-22} \text{ cm}^{-2} \text{ s}^{-1} \text{ sr}^{-1}$  is the full phase-space for 1 hour on the Moon, assuming an isotropic distribution for the cosmic rays or neutrinos and assuming the whole face of the Moon is in the antenna field of view. As in the previous section we have calculated the detection probability  $\mathcal{D}$  for a signal threshold of 500 Jy at all frequencies. It should be noted that for  $\nu = 30$  MHz there is a strong increase in the sky temperature and we have used a ten-fold higher threshold. As a result of the higher detection threshold the flux limit lies considerably higher.

From Fig. 3 one clearly sees that with decreasing frequency one loses sensitivity for lower-energy particles.

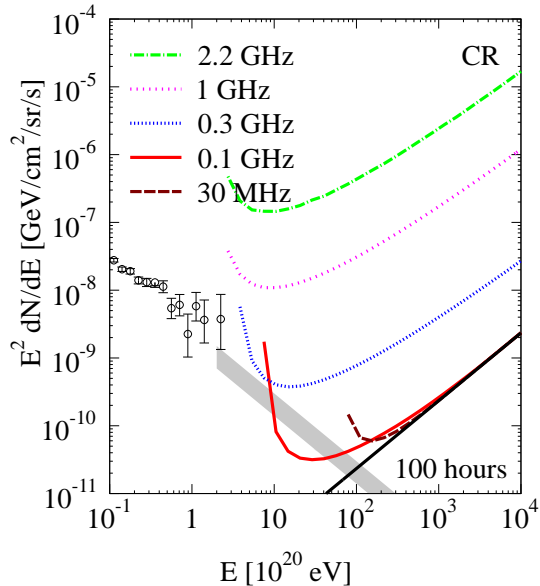


FIG. 3: Flux limits (assuming a null observation) for cosmic rays as can be determined in a 100 hour observation (see text). In the curves for  $\nu = 30$  MHz a ten fold higher detection threshold is used, corresponding to the higher sky temperature at this frequency. The points given correspond to the data of the AGASA experiment [28], the grey band is an extrapolation of the HiRes data [29]. The thick black line corresponds to the best possible limit (vanishing detection threshold).

This follows directly from Eq. (1) since with decreasing frequency the maximum signal strength decreases and thus one exceeds the detection threshold only for more energetic particles. If the energy of the cosmic ray is more than a factor 4 above this threshold value the analysis presented in the previous section applies and the detection limit improves rapidly with decreasing radio-frequency until one reaches a frequency of 100 MHz where one obtains the optimum sensitivity. Decreasing the frequency even lower provides no gain since the detection limit has already reached the optimum  $dN/dE_{opt} = Q/(0.5 \times h)$ , given by the heavy black line in Fig. 3.

In Fig. 4 we compare the detection limits for UHE neutrinos at different frequencies with the results obtained from the GLUE experiment [18]. One sees similar trends as in the predictions for cosmic rays, in particular the large gain in the determined flux limits with decreasing frequency. At higher energies the limits for neutrinos do not increase as steeply as those for cosmic rays. This is because the neutrino mean-free-path decreases with energy, therefore increasing the probability for the neutrino to initiate a shower close to the surface where the attenuation of the radio waves is small. Our result at 2.2 GHz happens to lie close to that of the GLUE experiment. The dashed-dotted curve in Fig. 4 shows the results of a calculation where we have reproduced the simulation for the GLUE experiment, i.e. included (in a somewhat

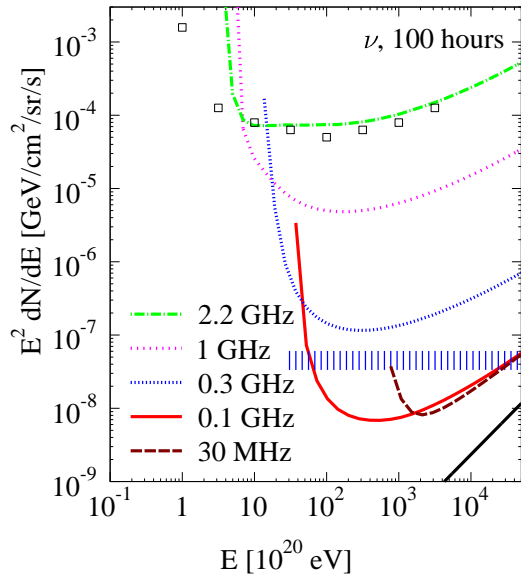


FIG. 4: Similar flux limits as shown in Fig. 3 but for UHE neutrinos. The open squares are the limits determined from the GLUE experiment [18].

simplified manner) the effects of averaging over lunar-surface slopes of  $10^\circ$ , including a 10% coverage of the Moon, and have used the appropriate detection threshold. This result lies close to the published limits of the GLUE experiment.

In this work we mainly address the detection limits for fluxes of UHE cosmic rays or neutrinos and a distinction between the two does not have to be made. When one would measure one or more events the question of distinguishing between the two kinds becomes interesting. For a single event the frequency dependence of the pulse (assuming a broad band acceptance) might give an indication since for deep showers the high-frequency part will suffer a larger attenuation than the low-frequency part. For a large number of events the distribution over the lunar surface could be exploited.

#### IV. WSRT & LOFAR PREDICTIONS

The Westerbork Synthesis Radio Telescope (WSRT) consists of fourteen 25 m parabolic dishes located on an east-west baseline extending over 2.7 km [35]. It is normally used for super-synthesis mapping, but elements of the array can also be coherently added to provide a response equivalent to that of a single 94 m dish. Observing can be done in frequency bands which range from about 115 to 8600 MHz, with bandwidths of up to 160 MHz. The low frequency band which concerns us here covers 115-170 MHz [36]. Each WSRT element has two receivers with orthogonal dipoles enabling measurement of all four Stokes parameters. In tied-array mode the system noise at low frequencies is  $F_{noise} = 600$  Jy. To observe radio

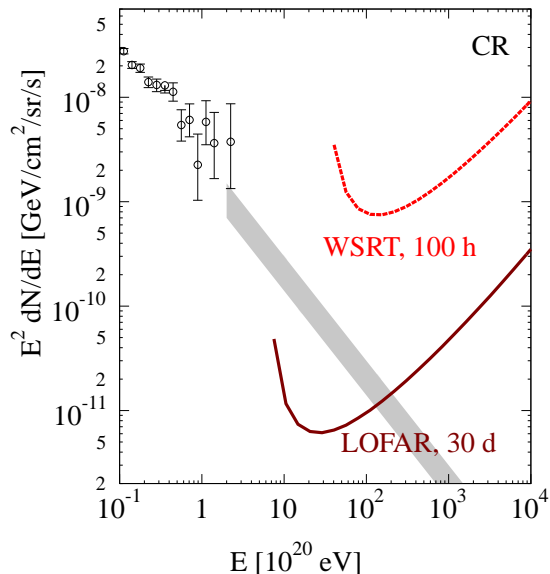


FIG. 5: Flux limits on UHE cosmic rays as can be determined in a 30 day observation with the LOFAR antenna system and a 100 hour observation with WSRT. The data shown are the same as in Fig. 3.

bursts of short duration, the new pulsar backend (PuMa II) will be used. It can provide dual-polarization base-band sampling of eight 20 MHz bands, enabling a maximum time resolution of approximately the inverse of the bandwidth. In the configuration which we propose to use, four frequency bands will observe the same part of the moon with the remaining four a different section. In total, coverage of about 50% of the lunar disk can be achieved.

An even more powerful telescope to study radio flashes from the moon will be the LOFAR array [37]. With a collecting area of about  $0.05 \text{ km}^2$  in the core (which can cover the full moon with an array of beams), LOFAR will have a sensitivity about 25 times better than that of the WSRT. LOFAR will operate in the frequency bands from 30-80 and 115-240 MHz where it will have a sensitivity of about  $F_{noise} = 600 \text{ Jy}$  and  $F_{noise} = 20 \text{ Jy}$ , respectively. The Galactic background noise will become the dominant source of thermal noise fluctuations at frequencies below about 100 MHz. It therefore appears that the optimal radio window for the detection of cosmic ray or neutrino induced radio flashes from the moon will be around 100-150 MHz.

The probability for a observing a signal simultaneously in four frequency bands with a power of  $20 \times F_{noise}$  per frequency band, where  $F_{noise}$  is the noise level per polarization direction, as a random fluctuation of the background noise is less than 0.001 (equal to  $3\sigma$  significance) for a 100 h observing period at a sampling rate of 40 MHz, typical for our PUMA-II back-end. Simulations show that a pulse of intensity  $25 \times F_{noise}$ , interfering with the noise background, can be detected with  $3\sigma$  signifi-

cance at a probability greater than 80%. For this reason we have assumed in the calculations a detection threshold of  $25 \times F_{noise}$  for both the WSRT and the LOFAR telescopes.

A simulation for LOFAR, taking  $\nu = 120 \text{ MHz}$ , bandwidth of  $\Delta\nu = 20 \text{ MHz}$ , a signal-detection threshold of 500 Jy, and an observation time of 30 days is shown in Fig. 5 for cosmic rays and in Fig. 6 for neutrinos. The results are compared with the limits that can be obtained from a presently proposed observation for 100 hours at the WSRT observatory assuming a detection threshold of 15,000 Jy,  $\nu = 140 \text{ MHz}$ , bandwidth of  $\Delta\nu = 20 \text{ MHz}$ , and a 50% Moon coverage.

In Fig. 6 the predicted spectrum of GZK neutrinos is taken from Ref. [31]. The prediction of top-down (TD) neutrinos is based on the decay of a topological defect with a mass of  $10^{24} \text{ eV}$  as was calculated in Ref. [7, 32]. The Waxman-Bahcall (WB) limit [30], based on theoretical arguments, is an upper limit on the neutrino flux which is consistent with the data on the fluxes of UHE cosmic rays. The limits are also compared with those from the GLUE [18] and FORTE [12] experiments which are calculated as model independent limits similar to our limits. The limit from the RICE [33] experiment has been calculated assuming different power-law spectra for the neutrinos. In general such a limit lies below the model-independent limit [12].

With the existing WSRT a limit on the neutrino flux can be set which falls just above the WB bound. However, even this will constrain different top-down scenarios, discussed in the literature. With the proposed LOFAR facility this limit can be improved considerably to reach, for the first time, a limit well below the WB bound for neutrinos. In addition one has a good chance to see evidence (in only a 30 day period) of cosmic ray events at an energy one order of magnitude higher than presently observed.

## V. ACCURACY OF THE PREDICTIONS

In this section we address the robustness of our acceptance calculations. Some of the sources of model-dependence in the calculation have already been discussed. A potentially large one is due to the uncertainty in the thickness of the regolith layer. As is argued in Appendix C, the final result is rather insensitive to this thickness since the rock below the regolith is as efficient, if not more so, in emitting radio-waves at the frequencies we are interested in.

The loss tangent of the regolith, which determines the attenuation of radio waves, is found to be dependent on the metallic composition of the regolith. Different Apollo samples show a large variation. The extremes for radio-attenuation distance in regolith vary between  $2/\nu \text{ m/GHz}$  to about  $25/\nu \text{ m/GHz}$  [24]. We have used an intermediate value of  $9/\nu \text{ m/GHz}$  for our estimates. As can be seen from Fig. 7 (please note the expanded scale) the

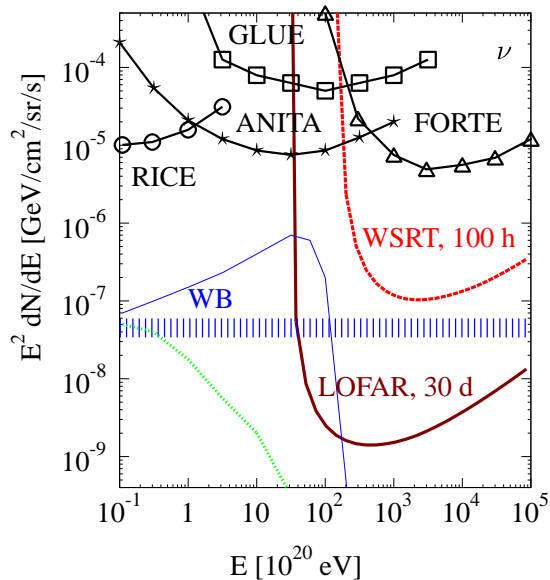


FIG. 6: Flux limits on UHE neutrinos as can be determined with WSRT and LOFAR observations (see text) are compared with various models, in particular, WB [30] (vertical bars), GZK [31] (dotted thin line), and TD [7, 32] (solid thin line). Limits from the RICE [33], GLUE [18], ANITA [34], and FORTE [12] experiments are also shown.

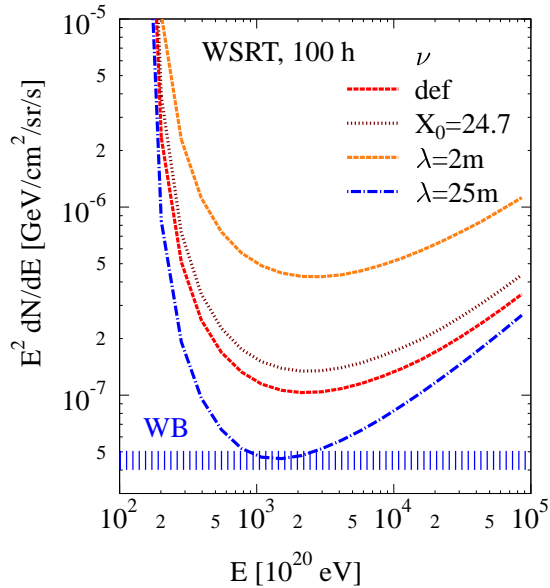


FIG. 7: Model dependence of flux limits on UHE neutrinos for WSRT. Note the different scale in this figure.

two extremes for the radio-absorption distance result in roughly a variation in the acceptance for neutrinos which is equal to the variation in the radio-attenuation length. The reason is that the thickness of the layer of the lunar crust which can be ‘seen’ on earth is proportional to the attenuation length of radio waves. It should be real-

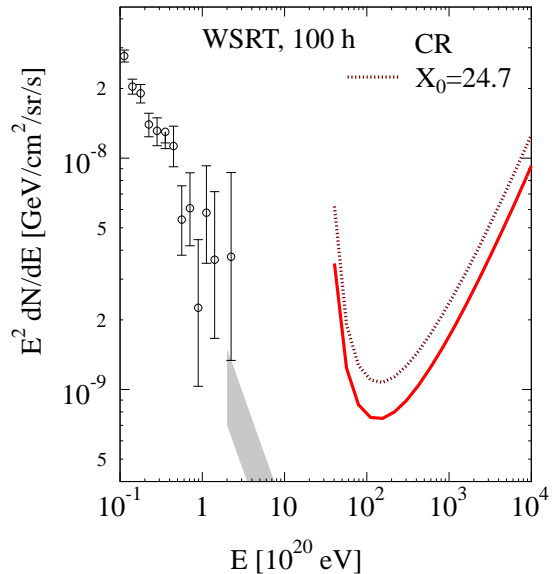


FIG. 8: Model dependence of flux limits on UHE cosmic rays for WSRT (and the LOFAR antenna system).

ized that the showers initiated by hadronic cosmic rays are close to the surface for which the exact value of the loss-tangent is unimportant.

We show in Appendix A that the angular spread of the emitted radio-waves from a shower depends on the length of the shower. This length is proportional to the stopping power  $X_0$ . As the stopping power is mostly determined by electronic processes it is strongly dependent on the elements in the rock or regolith. We have determined the stopping power for some of the Apollo samples analyzed in Ref. [43, 44]. This shows that the actual variation in the stopping power is not as large as one might have expected. We have determined  $X_0 = 22.1 \text{ g/cm}^2$  for the ‘A-17 HIGH Ti’ [43] sample which was used in the Monte Carlo simulations [27]. It is a typical Lunar Basalt and is similar to samples 70017, 70035 in ref. [44]. For the ‘A-15 Pyroxene’ [43] sample we determined  $X_0 = 23.2 \text{ g/cm}^2$  and  $X_0 = 24.7 \text{ g/cm}^2$  for some Apollo-16 samples [45]. In order to obtain an estimate of the sensitivity of the acceptance to the stopping power we also show in Fig. 7 the results of a calculation where the angular spread is reduced by a factor, equal to the reduction of the shower length,  $(24.7/22.1)$ . Since the detection limits are proportional to the third power of the angular spread, this results in only a 40% change.

An additional source of model dependence lies in principle in the details of modelling the roughness of the lunar surface. For the GLUE experiment, at much shorter wavelength, this roughness gave rise to a considerable broadening of the angular acceptance and thus to a large increase in the acceptance. Since, for the wavelength of interest for the LOFAR and WSRT telescopes, the angular spread is already large, the additional effects of surface roughness can be ignored as they give rise to only a

minor increase in the detection probability.

The Puma-II back-end which is available at the WRST telescope allows for storing all data on disk for each observation period. A total of 12 hours of observing time can be stored. The analysis of the data can thus be done off-line allowing full flexibility in optimizing the corrections for ionospheric dispersion. Because of the Nyquist sampling of the signal in the PUMA-II back-end the pulse may cover -after correction for dispersion- two to three sampling times. In the off-line analysis this can be taken into account. In the LOFAR operation the signal is also stored but only after a trigger condition is met in a fast on-line signal analysis.

## VI. SUMMARY

We have demonstrated the clear advantage of using radio waves at frequencies well below the Čerenkov maximum. The optimum frequency will be that where the length of the shower, of the order of several meters in the lunar regolith, is of the same order of magnitude as the wavelength of the radio waves where the radio-emission pattern is nearly isotropic. The advantage of going to lower frequencies applies to all experiments where the radiation crosses a boundary between a dense medium to one with a considerably lower index of refraction.

We have shown that the gain in efficiency at lower frequencies is such that with the upcoming LOFAR facility one can seriously investigate realistic top-down scenarios for UHE neutrinos and be sensitive to neutrino fluxes well below the Waxman-Bahcall limit. Even now with the existing WSRT, profiting from its capability to measure right in the radio-frequency window where the detection efficiency is highest, one is able to set limits on neutrino fluxes orders of magnitude below the present limit in only a 100 h observation period.

For UHE cosmic rays the LOFAR facility offers, because of the availability of an optimal radio-frequency window, a very powerful tool to determine the flux beyond the GZK limit. In only a 30 day observing period one is sensitive to a flux which is more than one order of magnitude below the extrapolation of the measured flux from below the GZK limit. Since the beam of LOFAR is determined by software, much longer observation periods should also be attainable, resulting in a sensitivity to even lower fluxes. Assuming the GZK limit is real, this offers the exciting possibility to measure the density of sources for UHE cosmic rays within a range of about 10 Mpc.

As an additional topic one may access the composition of cosmic-rays (proton versus heavy nuclei) by searching for the predicted coulomb dissociation of heavy nuclei passing in the neighborhood of the high density photon field of the Sun, the so called Gerasimova-Zatsepin effect [38]. The original predictions were recently revised [39], showing that the separation of the two dissociated daughter nuclei at 1 AU from the Sun is as large as

hundreds or even thousands of km, making the moon an excellent detector. The difference in the time of arrival of the two particles determines the mass of the original cosmic-ray nucleus.

## Acknowledgments

This work was performed as part of the research programs of the Stichting voor Fundamenteel Onderzoek der Materie (FOM) and of ASTRON, both with financial support from the Nederlandse Organisatie voor Wetenschappelijk Onderzoek (NWO). We gratefully acknowledge discussions with J. Alvarez-Muñiz on different aspects of shower development in dense media.

## APPENDIX A: ANGULAR SPREAD

Since the angular spread of the intensity of the Čerenkov radiation around the Čerenkov angle for the case  $\lambda \approx L$  is crucial for our considerations, we will present here a discussion of this case which is independent of the parameterizations given in the literature at shorter wavelength.

In the literature the intensity of Čerenkov radiation from a hadronic shower, with energy  $E_s$ , in the lunar regolith, in a bandwidth  $\Delta\nu$  at a frequency  $\nu$  and an angle  $\theta$ , has been parameterized, based on Monte Carlo simulations, as [11, 16, 18]

$$F(\theta, \nu, E_s) = 3.86 \times 10^4 e^{-((\theta-\theta_c)/\Delta_c)^2} \left(\frac{d_{moon}}{d}\right)^2 \times \left(\frac{E_s}{10^{20} \text{ eV}}\right)^2 \left(\frac{\nu}{\nu_0(1+(\nu/\nu_0)^{1.44})}\right)^2 \times \left(\frac{\Delta\nu}{100 \text{ MHz}}\right) \text{ Jy}, \quad (\text{A1})$$

where  $\nu_0 = 2.5$  GHz and the spreading  $\Delta_c$  is given by Eq. (3). Eq. (A1) has been experimentally shown [10] to be accurate within a factor 2 for a shower of particles that would correspond to a primary particle of about  $10^{19}$  eV at frequencies exceeding 1 GHz where the wavelength is small compared to the longitudinal extent (length) of the shower. For the case in which the wavelength is comparable to the length of the shower, of interest for the present investigation, one may expect deviations from the simple parametrization where our main concern is the angular spread of the Čerenkov radiation.

To focus on the angular spread, we have derived the angular distributions for two different shower profiles following the approach given in [12]. For the first one, called the “block” profile, the number of charged particles is constant over the shower length  $L = L_b$ ,  $\rho_b(x) = 1$  for  $0 < x < L_b$ . This profile is not realistic for a shower as the full intensity suddenly appears and disappears. For this reason we have also investigated a second profile where the charge in the shower appears and disap-

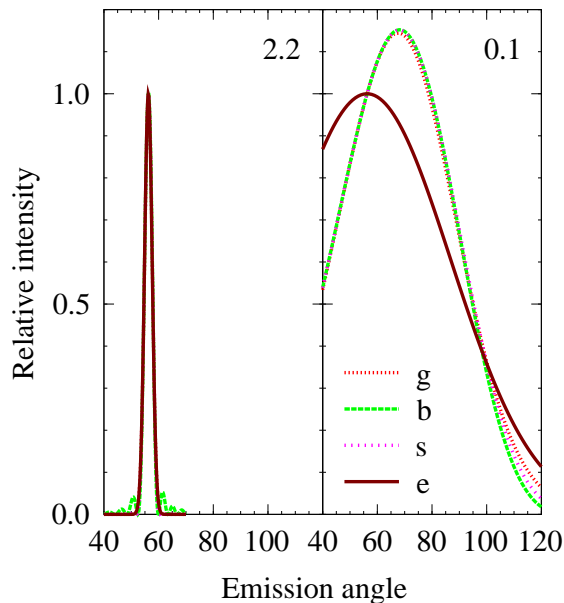


FIG. 9: The angular spread around the Čerenkov angle for the block and the sine shower-profile functions are compared to the parametrization used in this work (e: Eq. (A1); g: Eq. (A5); b: Eq. (A2); s: Eq. (A4)). The left (right) hand displays the results for 2.2 GHz (100MHz) respectively.

pears following a sine profile,  $\rho_s(x) = \sin \pi x/L_s$  with  $0 < x < L_s$ .

For the block longitudinal profile we reproduce the well known intensity distribution found by Tamm [47] for a finite length shower, normalized to unity at the Čerenkov angle,

$$I_b(\theta) = \left[ \frac{\sin \theta}{\sin \theta_c} \frac{\sin \pi \chi}{\pi \chi} \right]^2 \quad (\text{A2})$$

with

$$\chi = (\cos \theta - 1/n)L/\lambda \quad (\text{A3})$$

For the normalized “sine” profile we obtain

$$I_s(\theta) = \left[ \frac{\sin \theta}{\sin \theta_c} \frac{\cos \pi \chi}{(1 - 2\chi)(1 + 2\chi)} \right]^2 \quad (\text{A4})$$

The predictions of these two formulas are compared with the parametrization of Eq. (A1) at 2.2 GHz and 100 MHz for a shower of  $10^{20}$  eV. To reproduce the angular spread of this calculation at 2.2 GHz we choose  $L_b = 2.5$  m and  $L_s = L_b \times 4/3 = 3.4$  m, see Fig. 9. The results are also compared to those of the gaussian parametrization proposed in [12],

$$I_s(\theta) = \left[ \frac{\sin \theta}{\sin \theta_c} \right]^2 e^{-Z^2}, \quad (\text{A5})$$

with  $Z$  given by Eq. (A7). The value for  $Z_0$ , Eq. (A8), is chosen such that for a small angle expansion around  $\theta_c$  it agrees exactly with Eq. (A1). From the figure it is

seen that the simple parametrization of Eq. (A1) is reproduced well by all three analytic forms. Eq. (A2) shows the well known secondary interference maxima, due to the sharp edges of the profile [40], which are not realistic for our case. Keeping parameters fixed the angular distributions are now compared at 100 MHz (right hand panel of Fig. 9). The three analytic forms, Equations (A2), (A4), and (A5) agree quite accurately but differ considerably from Eq. (A1). The reason for this difference lies mainly in the pre-factor  $\sin^2 \theta$ , missing in Eq. (A1), which accounts for the radiation being polarized parallel to the shower and thus that emission at  $0^\circ$  and  $180^\circ$  is not possible.

On the basis of the arguments given above we will use the gaussian parametrization, accurate at small and large angles,

$$F(\theta, \nu, E_s) = 3.86 \times 10^4 e^{-Z^2} \left( \frac{\sin \theta}{\sin \theta_c} \right)^2 \left( \frac{d_{moon}}{d} \right)^2 \quad (\text{A6}) \\ \times \left( \frac{E_s}{10^{20} \text{ eV}} \right)^2 \left( \frac{\nu}{\nu_0(1 + (\nu/\nu_0)^{1.44})} \right)^2 \left( \frac{\Delta \nu}{100 \text{ MHz}} \right)^2 \text{Jy},$$

with

$$Z = (\cos \theta - 1/n)Z_0. \quad (\text{A7})$$

The value for

$$Z_0 = \left( \frac{n}{\sqrt{n^2 - 1}} \right) \left( \frac{180}{\pi \Delta_c} \right), \quad (\text{A8})$$

with  $\Delta_c$  measured in degrees (see Eq. (3)). For small spreading angles around the Čerenkov angle, i.e. short wavelengths, this expression agrees with the results of Monte Carlo simulations [11, 16, 18] while at large wavelengths the formula agrees with the analytic results [42].

As a last point we compare the length of the shower, 1.7 m according to Eq. (4), with the value for the length used in Eq. (A4),  $L_s = 3.4$  m. It should be realized that for the sine profile, only for half its length (i.e. 1.7 m) the density of charged particles exceeds 70% of the maximum value, which is the definition of the shower length in the Monte-Carlo simulations. The agreement is thus excellent.

## APPENDIX B: SHALLOW SHOWERS

In this paper we have implicitly assumed that the showers develop well inside the lunar regolith. For the emission of long wavelength radio waves from cosmic ray showers which are close to the lunar surface this assumption needs a more detailed consideration. The proximity of the surface, through mechanisms like mirror charges, could severely diminish the amount of Čerenkov radiation through the surface.

Even though the general problem has not been studied, the -in some sense- inverse problem has been studied [46], namely that of an electron beam in close proximity to a

dielectric. When the velocity of the electrons exceeds that of the velocity of light in the medium ( $c_m = c/n$ , where  $n$  is the index of refraction) Čerenkov radiation is induced in the medium. The occurrence of this process has been verified experimentally [41]. In Ref.[46] the amount of Čerenkov radiation is calculated as a function of all key parameters in the problem such as the distance  $a$  of the electron beam from the surface, the electron velocity  $\beta = v/c$ , the wavelength of the radiation  $\lambda$ , and the angle  $\eta$  of the radiation with respect to the surface of the dielectric. In the limit of ultra-relativistic particles ( $\beta = 1$ ) the dependence of the intensity on  $a$  reads

$$W \sim e^{-4\pi a\sqrt{n^2-1}/\lambda}. \quad (\text{B1})$$

This equation differs from that quoted in [41] where instead the limit  $\beta \gtrsim 1/n$  has been used. Eq. (B1) clearly shows that proximity of the surface is only an issue when  $4\pi a\sqrt{n^2-1}/\lambda \lesssim 1$  or for  $a \lesssim \lambda/(4\pi\sqrt{n^2-1}) = 0.05\lambda$  for the lunar regolith. This implies that this effect should be considered only for showers making very small angles to the surface, i.e. “shallow showers” with  $\sin\theta \lesssim 0.05\lambda/(0.5L)$ , where  $L$  is the shower length. For  $L = \lambda$  this corresponds to an angle of less than  $6^\circ$ .

To test the contribution of shallow showers to our results we have made calculations in which the contribution of shallow showers are excluded. The difference in the results is barely visible in the plots and this effect can thus safely be ignored.

It should however be realized that it is only an extrapolation to apply the conclusions based on the work of Ref.[46] to the present problem. A thorough theoretical treatment should be performed.

### APPENDIX C: LUNAR REGOLITH

The properties of the regolith play an important role in the present calculations. The index of refraction and the loss tangent (determining the attenuation length of radio waves) have been determined from samples brought back to Earth in the Apollo missions. From the average values one extracts an index of refraction of  $n = 1.8$  and an attenuation length of  $\lambda_r = (9/\nu[\text{GHz}])$  m [24, 48] for the intensity of radio waves in regolith.

One issue of particular interest for the detection efficiency of neutrino-induced showers is the thickness of the regolith. In his thesis [49] Takahashi made an extensive study of the absorption and reflection of radio waves in the frequency domain of 0.1 to 10 MHz for realistic depth profiles based on [48]. He expects a smoothly varying attenuation length of  $\lambda_r = 4.08(\nu[\text{GHz}])^{-.81}$  m for depths ranging from 200 m up to 100 km. At these depths one expects a decreased attenuation length due to the increased density of the material. Since the density of rock is about twice as high as that of the regolith also the value of the index of refraction (and thus the Čerenkov angle) and the length of hadronic shower (and

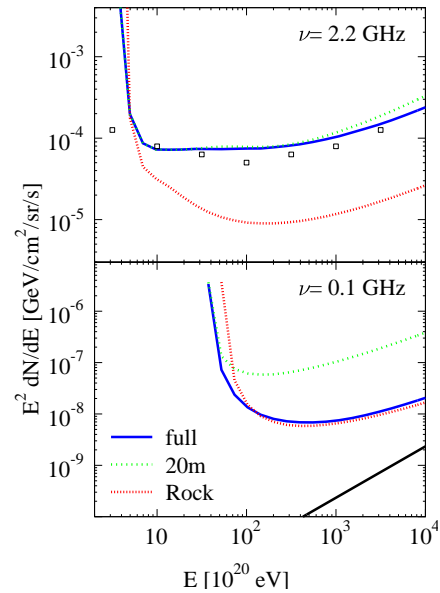


FIG. 10: The dependence of the detection limits on properties of the lunar regolith. The solid curve represents a calculation made as if the regolith extends to a depth of 500 m, with only 20 m assumed for the dotted curve, while pure lunar rock is taken for the short dashed calculation.

thus the spread around the Čerenkov angle) should be modified. To study these different effects we compare in Fig. 10 the results of three different calculations. In the first (the solid curve) we assume that the properties of the regolith layer apply to depths of 500 m. In the second (dotted curve) the regolith extends to a depth of 20 m and we assume that no radiation from deeper layers reaches the surface. In the third calculation we assume that the lunar rock extends to the surface of the moon. The density of the rock is taken twice that of the regolith, the index of refraction equal to 2.6, the radio absorption length equal to one third of that of the regolith, which takes into account the larger value of the loss tangent in rock.

At a frequency of 2.2 GHz one finds, by comparing the drawn and the dashed curves, that only showers in the upper part of the regolith are detectable due to the relatively strong absorption of radio waves. At this frequency the detectability of showers in rock is much higher due to the fact that the spread around the Čerenkov angle is twice as large due to the reduced length of the shower which in turn is a consequence of the larger density. However the rock is at most areas covered by a layer of regolith which will completely attenuate the radio waves. The calculations for 20 or 500 m of regolith (hardly any difference between the two) thus yield a conservative lower limit. At 100 MHz the situation is quite different. The calculations for pure rock or pure regolith give rise to very similar limits. The increase in spreading width for the calculation in rock is apparently compensated by an increased attenuation. Due to the larger

wavelength the contribution of showers deep under the surface are important. If only the showers in the upper 20 m of regolith are taken into account in the calculation, the limit changes by about 1 order of magnitude. This calculation completely ignores the emission from deeper showers which is clearly unrealistic. If one adds the contribution from the deeper rock layer one will obtain a result close to the drawn curve. Including the fact that for rock covered by a layer of regolith the index of refraction changes more gradually, giving rise to reduced reflection

near the surface, would even give a more stringent lower limit. Again, the calculation taking a maximum depth of 500 m gives a realistic estimate for the limit.

The calculations in the main part of this work account for radiation emitted from a depth of not more than 500 m. On the basis of the arguments presented in the above it will be clear that this gives a realistic estimate for lower bounds on neutrino fluxes. For cosmic rays none of these considerations are important as all induced showers lie in the upper part of the regolith.

- 
- [1] K. Greisen, Phys. Rev. Lett. **16**, 748 (1966).  
 [2] G.T. Zatsepin, V.A. Kuzmin, Pis'ma Zh. Eksp. Teor. Fiz. **4**, 114 (1966), [JETP. Lett. **4**, 78 (1966)].  
 [3] A. Achterberg, Y.A. Gallant, J.G. Kirk, A.W. Guthmann, MNRAS**328**, 393 (2001).  
 [4] O. Deligny, A. Letessier-Selvon, E. Parizot, Astropart. Phys. **21**, 609 (2004).  
 [5] P. Bhattacharjee, U. Sigl, Phys. Rep. **327**, 109 (2000).  
 [6] S. Yoshida, H. Dai, C. C. H. Jui, and P. Sommers, Astrophys. J. **479**, 547 (1997); P. Bhattacharjee, C.T. Hill, and D. N. Schramm, Phys. Rev. Lett. **69**, 567 (1992).  
 [7] Todor Stanev, astro-ph/0411113.  
 [8] S. Sarkar and R. Toldra, Nucl. Phys. **B621**, 495 (2002).  
 [9] G. A. Askaryan, Sov. Phys. JETP **14**, 441 (1962); **21**, 658 (1965).  
 [10] D. Saltzberg et al., Phys. Rev. Lett. **86**, 2802 (2001); P.W. Gorham et al., Phys. Rev. **E62**, 8590 (2000).  
 [11] E. Zas, F. Halzen, and T. Stanev, Phys. Rev. D **45**, 362 (1992); J. Alvarez-Muñiz and E. Zas, Phys. Lett. B **411**, 218 (1997).  
 [12] N.G. Lehtinen, P.W. Gorham, A.R. Jacobson and R.A. Roussel-Dupre, Phys. Rev. D **69**, 013008 (2004); note that an obvious square is missing for the  $\Delta\theta$  term in Eq. 1.  
 [13] P. Miočinović, for the ANITA Collaboration, astro-ph/0503304; 22nd Texas Symposium on Relativistic Astrophysics at Stanford University, (2004).  
 [14] D. Saltzberg et al., Proc. SPIE **4858**, 191 (2003); M. Chiba, T. Kamijo, O. Yasuda, et al., Phys. Atom. Nuclei **67**, 2050 (2004); P. Gorham, D. Saltzberg, A. Odian, et al., NIM **A490**, 476 (2002).  
 [15] R. D. Dagkesamanskii and I.M. Zheleznyk, Sov. Phys. JETP **50**, 233 (1989).  
 [16] J. Alvarez-Muñiz, R. A. Vazquez, and E. Zas, Phys. Rev. D **61**, 23001 (99); J. Alvarez-Muñiz and E. Zas, astr-ph/0102173, in "Radio Detection of High Energy Particles RADHEP 2000", AIP Conf. Proc. No. 579 (AIP, New York, 2001).  
 [17] T. H. Hankins, R. D. Ekers, and J. D. OSullivan, Mon. Not. R. Astron. Soc. **283**, 1027 (1996).  
 [18] P. Gorham et al., Phys. Rev. Lett. **93**, 41101 (2004).  
 [19] H. Falcke and P. Gorham, Astropart. Phys. **19**, 477 (2003).  
 [20] D.A. Suprun, P.W. Gorham, J.L. Rosner, Astropart. Phys. **20**, 157 (2003).  
 [21] T. Huege and H. Falcke, Astropart. Phys. **24**, 116 (2005).  
 [22] H. Falcke et al., Nature **435**, 313 (2005).  
 [23] D. Ardouin et al., Proceedings of the 29<sup>th</sup> Int. Cosmic ray Conf., Pune, India (2005), astro-ph/0510170.  
 [24] G.R. Olhoeft and D.W. Strangway, Earth Plan. Sci. Lett. **24**, 394 (1975).  
 [25] R. Gandhi, Nucl. Phys. B **91**, 453 (2000).  
 [26] 600 Jy corresponds to the noise level used in the analysis of the GLUE experiment [18] and also to the noise level of the WSRT array (see discussion in Section IV).  
 [27] J. Alvarez-Muñiz and E. Zas, Phys. Lett. B **434**, 396 (1998). Calculations are for sample 'A-17 HIGH Ti' of ref. [43].  
 [28] M. Takeda et al., Astropart. Phys. **19**, 447 (2003); <http://www.akeno.icrr.u-tokyo.ac.jp/AGASA/>  
 [29] R.U. Abbasi et al., Phys. Rev. Lett. **92**, 151101 (2004).  
 [30] J. Bahcall and E. Waxman, Phys. Rev. D **64**, 64 (2001).  
 [31] R. Engel, D. Seckel, T. Stanev, Phys. Rev. D **64**, 93010 (2001).  
 [32] R.J. Protheroe, T. Stanev, Phys. Rev. Lett. **77**, 3708 (1996).  
 [33] RICE Collaboration, I. Kravchenko et al., Astropart. Phys. **20**, 195 (2003).  
 [34] S.W. Barwick et al., Phys. Rev. Lett. **96**, 171101 (2006).  
 [35] J.W.M. Baars, B.G. Hooghoudt, Astron. & Astrophys. **31**, 323 (1974).  
 [36] A.G. de Bruyn, E.M. Woestenburg, J. van der Marel, "Observing at low frequencies with the WSRT", in "Astronews", July 2005 (<http://www.astron.nl/>).  
 [37] J.D. Bregman, Proceedings of the SPIE, **4015**, 19 (2000); H. Butcher, Proceedings of the SPIE, **5489**, 537 (2004); see also <http://www.lofar.org/>.  
 [38] N.M. Gerasimova and G.T. Zatsepin, Soviet Physics JETP **11** (1960) 899.  
 [39] G.A. Medina-Tanco and A. Watson, Astropart. Physics **10** (1999) 157.  
 [40] R.V. Buniy and J.P. Ralston, Phys. Rev. D **65**, 016003 (2001).  
 [41] T. Takahashi et al., Phys. Rev. **E62**, 8606 (2000).  
 [42] see also J. Alvarez-Muñiz et al., astro-ph/0512337.  
 [43] Arden L. Albee, "Lunar Rocks" in the Encyclopedia of Astronomy and Astrophysics, 1973.  
 [44] The Lunar Sample Compendium, Compiled by Charles Meyer, Lyndon B. Johnson Space Center (JSC-62905) Houston, Texas, see <http://www.curator.jsc.nasa.gov/lunar/references.cfm>.  
 [45] R.L. Korotev, Met. Plan. Sci. **32**, 447 (1997).  
 [46] R. Ulrich, Z. Phys. **194**, 180 (1966). We used eq. 18 of this work.  
 [47] I.E. Tamm, J. Phys. (Moscow) **1**, 439 (1939).  
 [48] G. Heiken, D. Vaniman, and B. M. French, "Lunar Sourcebook, A Users Guide to the Moon", ISBN

0521334446, Cambridge University Press, 1991.

- [49] Yuki David Takahashi, “New Astronomy from the Moon: A Lunar Based Very Low Frequency Radio Array”, MsSc

Thesis, University of Glasgow, 2003.